

Figure S1. Pathological analysis of lung tissues in SARS-CoV-2-challenged mice. (A) Representative hematoxylin and eosin (HE) staining of lung tissues harvested on day 5 post-challenge from mice in **Figure 4A**. Inflammation (arrows, top row) and edema in airspaces (asterisks, bottom row) were much more evident in the control group (two left panels) compared to the treatment group (two right panels). **(B)** Representative HE staining of lung tissues harvested on day 5 post-challenge from mice in **Figure 4B**. The control group (two left panels) shows much more evident cellular perivascular cellular aggregates (arrows) and smaller airspaces compared to the treatment groups (two right panels).

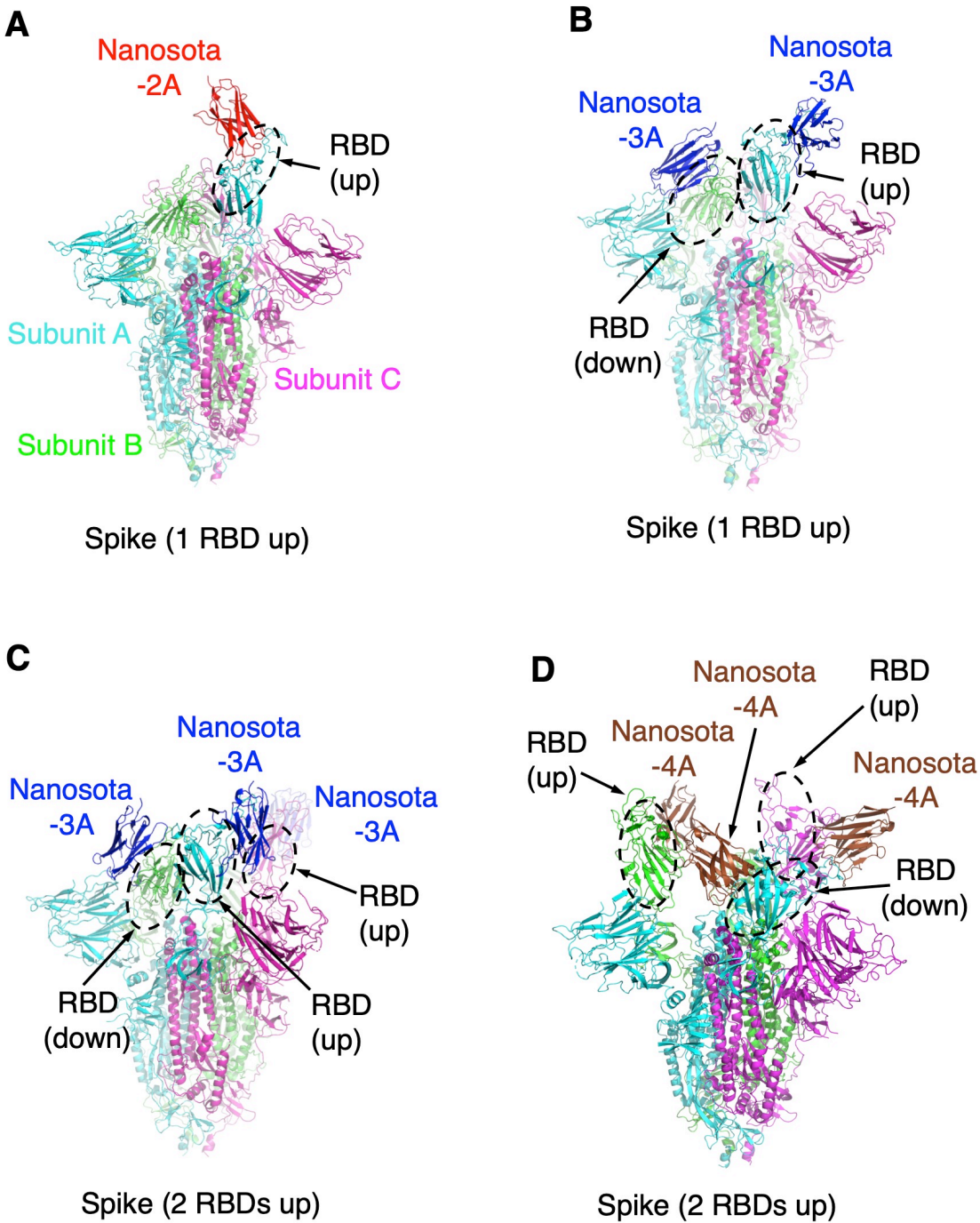


Figure S2. Structures of prototypic SARS-CoV-2 spike complexed with either Nanosota-2A, -3A or -4A. (A) SARS-CoV-2 spike (with one RBD up) complexed with Nanosota-2A. (B) SARS-CoV-2 spike (with one RBD up) complexed with two Nanosota-3A molecules. (C) SARS-CoV-2 spike (with two RBDs up) complexed with three Nanosota-3A molecules. (D) SARS-CoV-2 spike (with two RBDs up) complexed with three Nanosota-4A molecules. The spike trimer is colored by different subunits: subunit A in cyan, subunit B in green and subunit C in magenta.

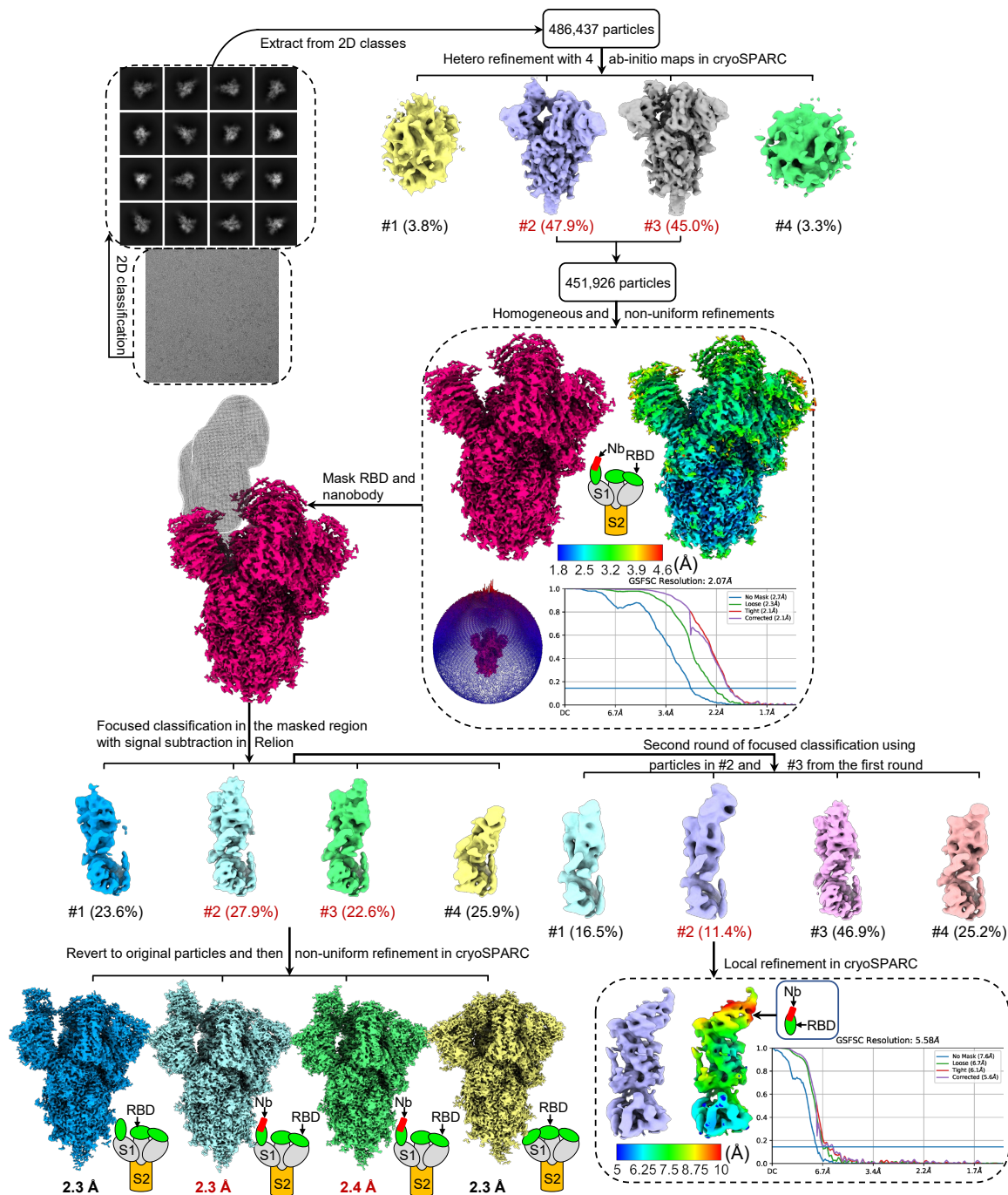


Figure S3. Flow chart of cryo-EM image processing and 3D reconstruction for prototypic SARS-CoV-2 spike/Nanosota-2A complex. Representative raw cryo-EM image and 2D classes are presented. 3D refinements using all the particles from good 3D classes generated a 2.1 Å map. Two rounds of masked 3D classification and further local refinement visualized the density for the bound nanobody. Angular distribution plot, the final maps, half-map FSC curves and accompanying local resolution illustrations are enclosed in the dashed black boxes.

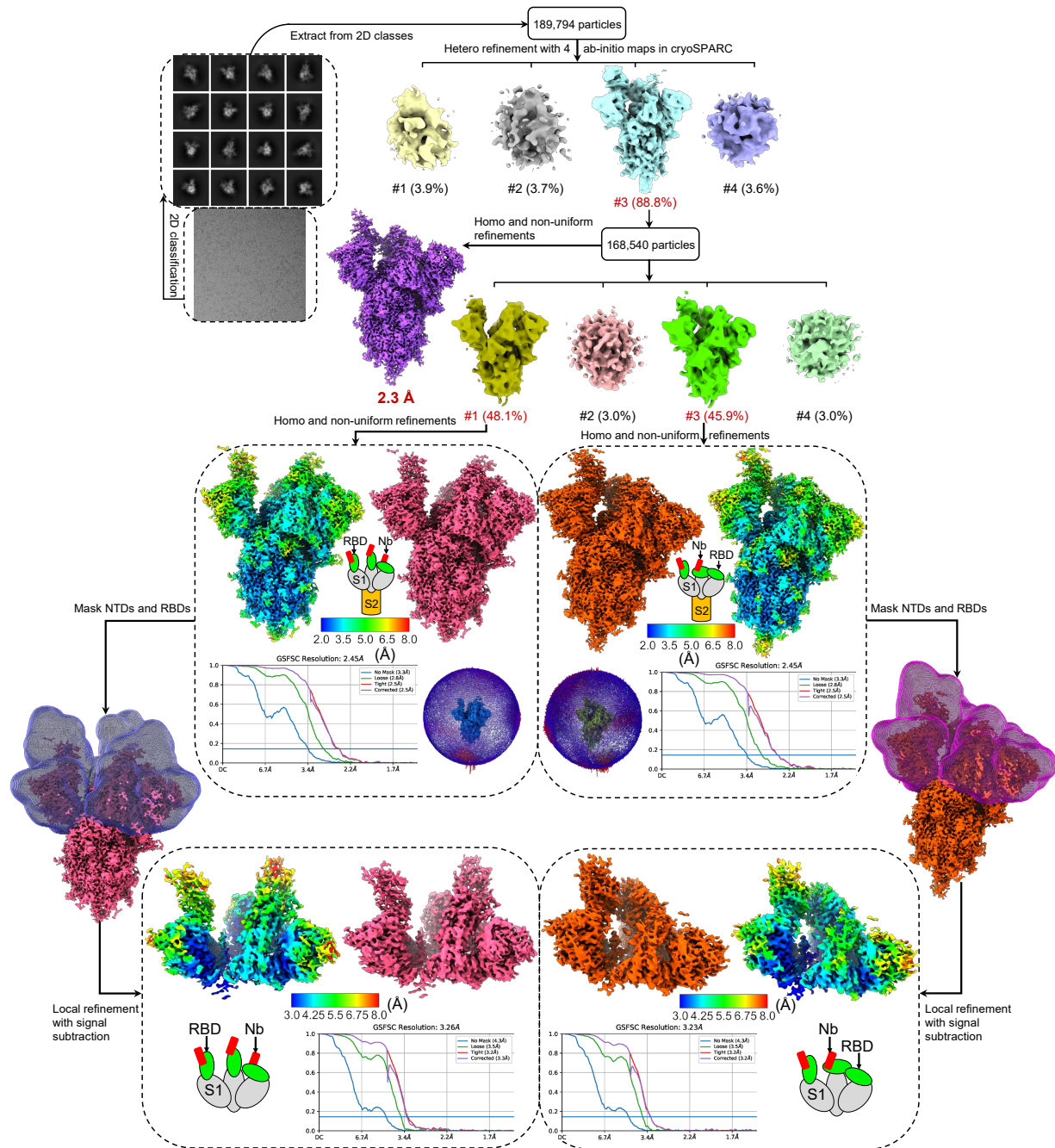


Figure S4. Flow chart of cryo-EM image processing and 3D reconstruction for prototypic SARS-CoV-2 spike/Nanosota-3A complex. Representative raw cryo-EM image and 2D classes are presented. 3D refinements using the particles from individual good 3D classes generated 2.5 Å maps. Further local refinements improved the density for the bound nanobodies. The final maps, half-map FSC curves, angular distribution plot and accompanying local resolution illustrations are enclosed in the dashed black boxes.

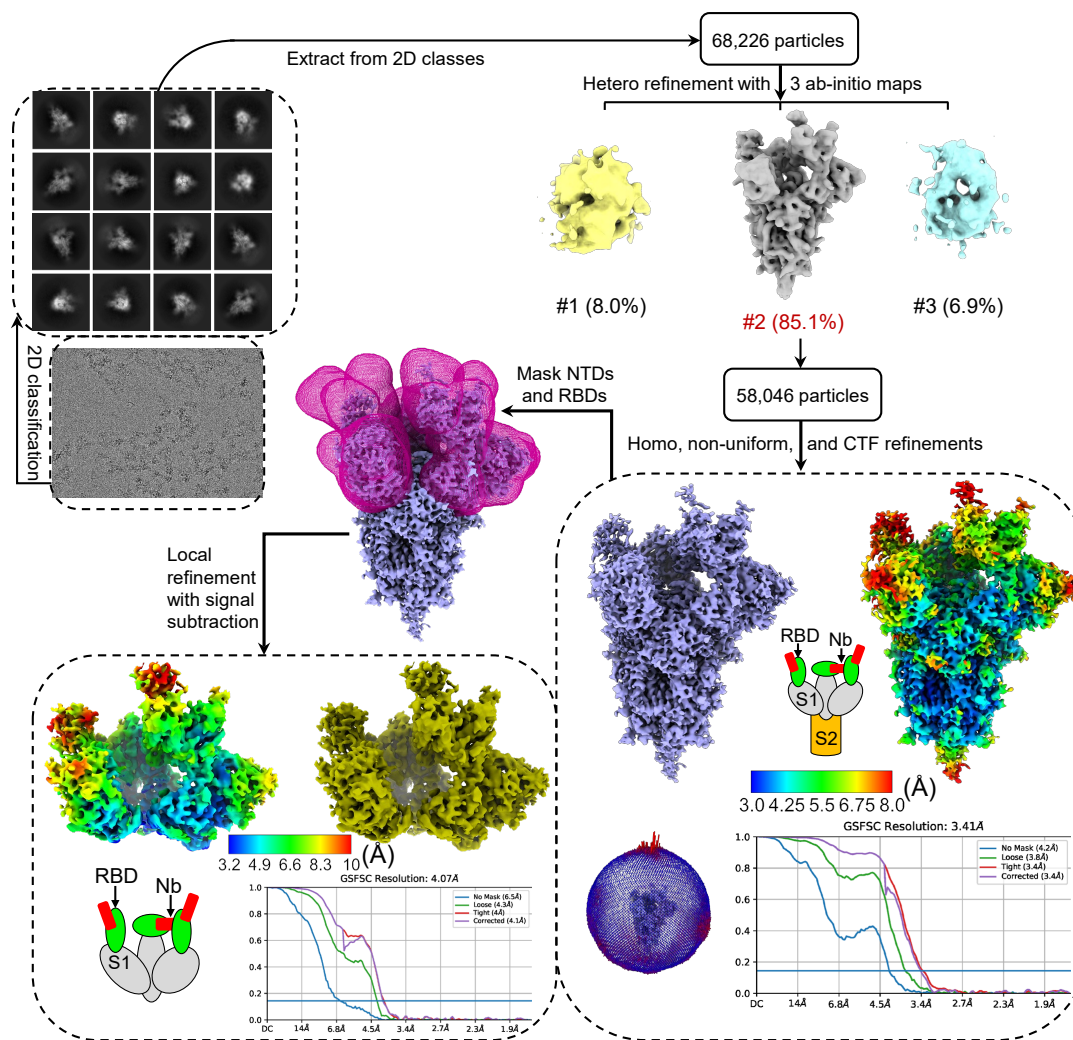


Figure S5. Flow chart of cryo-EM image processing and 3D reconstruction for prototypic SARS-CoV-2 spike/Nanosota-4A complex. Representative raw cryo-EM image and 2D classes are presented. 3D refinements using the particles in the good 3D class generated a 3.4 Å map. Further local refinements improved the density for the bound nanobodies. The final maps, half-map FSC curves, angular distribution plot and accompanying local resolution illustrations are enclosed in the dashed black boxes.

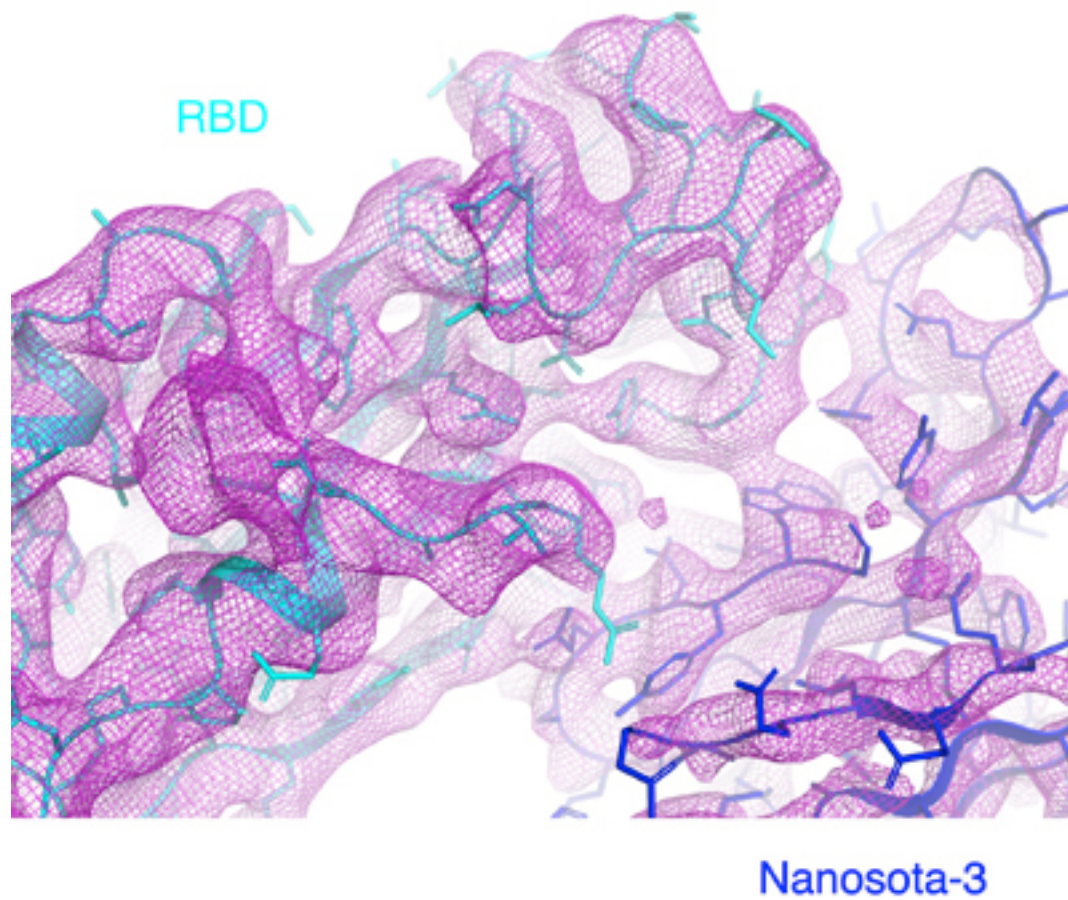


Figure S6. Cryo-EM densities (after local refinement) of the interface between the lying-down RBD and Nanosota-3A. RBD is colored in cyan, Nanosota-3A is colored in blue, and cryo-EM densities are colored in magenta.

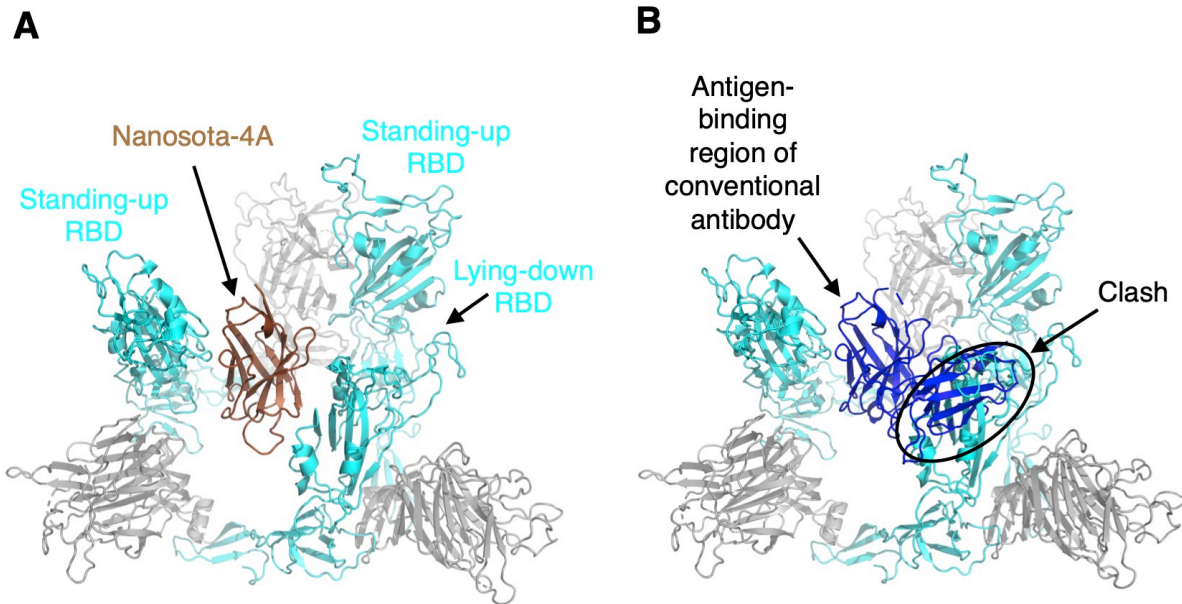


Figure S7. Nanosota-4A fits into a cavity in the trimeric spike, which would not accommodate conventional antibodies. (A) Nanosota-4A (consisting of only the heavy chain) binds to the lying-down RBD by fitting into a cavity in the trimeric spike. Only the three receptor-binding subunits are shown. RBD is colored in cyan. Nanosota-4A is colored in brown. **(B)** The antigen-binding region (consisting of both heavy and light chains) of a conventional antibody (PDB 7DEO) would not fit into the cavity and hence would not bind to the lying-down RBD in the same way as Nanosota-4A does. The clash of the antibody and the spike protein is labeled.

Table S1. *In vitro* anti-SARS-CoV-2 potency of antibodies/nanobodies from the literature

Reference	Nanobody	Conventional antibody	Pseudovirus	Live virus	Animal testing?
Current study	Nanosota-2A-Fc		0.50 ng/ml = 6.2 pM (WT) 0.56 ng/ml = 6.9 pM (Alpha) 1.1 ng/ml = 14 pM (Delta)	0.16 ng/ml = 2 pM (WT)	Yes
Current study	Nanosota-3A-Fc		5.7 ng/ml = 74 pM (WT) 1.2 ng/ml = 16 pM (Alpha) 3.6 ng/ml = 47 pM (Omicron)	2.3 ng/ml = 30 pM (Omicron)	Yes
(1)		A23-58.1, B1.182.1	0.3-11 ng/ml (23 variants; no Omicron)	2.1-4.8 ng/ml (WT)	No
(2)		35B5		1.6 ng/ml (WT)	Yes
		32C7		8.6 ng/ml (WT)	
(3)		J08, I14		1-10 ng/ml (D614G, Alpha)	Yes
(4)		JMB2002	150 ng/ml (omicron)		No
(5)		35B5	2.4 ng/ml (Delta) 6.9 ng/ml (Delta) 15 ng/ml (Omicron)	50 ng/ml (Omicron)	No
(6)		S2E12	1.4 ng/ml (WT) 38 ng/ml (Omicron)		No
		LY-CoV1404	3.0 ng/ml (WT) 5.1 ng/ml (Omicron)		
(7)		P17	165 pM (WT)	195 pM (WT)	Yes
(8)		Clone2	0.54 ng/ml (WT);37.8 ng/ml (Beta)	7.70 ng/ml (WT); 31.51 ng/ml (Delta)	Yes
		Clone6	4.2 ng/ml (WT);435.8 ng/ml (Beta)	6.14 ng/ml (WT); 111.34 ng/ml (Delta)	
		Clone13A	6.2 ng/ml (WT)	59.28 ng/ml (WT); 120.10 ng/ml (Delta)	Yes
(9)		STE90-C11		0.56 nM (WT)	Yes
(10)		WRAIR NTD mAbs	6-27 ng/ml (WT)	32-215 ng/ml (WT)	Yes
		WRAIR RBD mAbs	4-17 ng/ml (WT)	33-172 ng/ml (WT)	
(11)		31 RBD mAbs	2-800 ng/ml (WT, Alpha, Beta, Gamma, Delta, Lambda); < 20 ng/ml (Omicron)		Yes
(12)	Nanosota-1C-Fc		0.27 ug/ml (WT)	0.16 ug/ml (WT)	Yes
(13)	ANTE-CoV2-Nab21T _{GS}		1.32 pM (WT)	6.04 pM (SARS-CoV-2 Munich strain)	No
(14)	mNb6-tri		5.0 ng/ml = 120 pM (WT)	2.3 ng/ml = 54 pM (WT)	No
(15)	C5-Trimer			20 pM (WT) 25 pM (Alpha)	Yes

(16)	Nb 19 trimer		0.7 ng/ml = 9 pM (WT)		No
	Nb 56 trimer		3.9 ng/ml = 55 pM (WT)	0.2 ng/ml = 3 pM (WT) 0.6 ng/ml = 8 pM (Alpha) 1.3 ng/ml = 18 pM (Beta) 0.2 ng/ml = 3 pM (Gamma)	
(17)	WNb-Fc 36			100 pM (WT) 110 pM (N501Y; D614G)	Yes
(18)	aRBD-2-5-Fc		20 pM (Omicron)	83 pM (WT) 44 pM (Beta) 27 pM (Delta) 29 pM (Omicron)	Yes
(19)	8A2+7A3		1 nM (WT) 400 pM (Alpha) 300 pM (Beta) 200 pM (Gamma)	1 nM (WT) 6 nM (614G) 2 nM (Alpha) 870 pM (Beta) 140 pM (Gamma) 19 nM (Delta)	Yes
(20)	2-67(A)		80 pM (WT) 80 pM (Alpha) 180 pM (Delta) 110 pM (Omicron)	310 pM (Delta)	No
(21)	V _H -Fc ab8		30 ng/ml (WT)	40 ng/ml (WT)	Yes
(22)	humVHH_S56A/LAL APG-Fc/Gen2			110 ng/ml (Beta)	Yes
	(humVHH_S56A)2/L ALAPG-Fc/Gen2			20 ng/ml (Beta)	
(23)	BP10-Fc			90 ± 20 nM (WT)	Yes
	BP19-Fc			112 ± 18 nM (WT)	
	BP39-Fc			34 ± 2 nM (WT)	
(24)	BiShAb0201		24 ng/ml (WT) 26 ng/ml (Beta) 5 ng/ml (Delta) 27 ng/ml (BA.1) 35 ng/ml (BA.5)		Yes
	ShAb01H02K		< 23 ng/ml (WT) 21 ng/ml (Beta) 2 ng/ml (Delta) 391 ng/ml (BA.1) 524 ng/ml (BA.5)		

(25)	MR14		5.3 ± 0.45 ng/ml (WT) 5.0 ± 1.7 ng/ml (Delta) 0.16 ± 0.044 ng/ml (BA.1) 0.17 ± 0.082 ng/ml (BA.2) 0.69 ± 0.63 ng/ml (BA.3) 18.7 ± 9.7 ng/ml (BA.4/5)	91 ng/ml (WT) 13 ng/ml (Delta) 6.6 ng/ml (BA.1) 3.4 ng/ml (BA.2)	Yes
	MS43		179 ± 7.4 ng/ml (WT) 30 ± 17 ng/ml (Delta) 1.5 ± 0.037 ng/ml (BA.1) 52520 ± 43208 ng/ml (BA.2) 50 ± 25 ng/ml (BA.3) 4405 ± 2672 ng/ml (BA.4/5)	1117 ng/ml (WT) 20 ng/ml (Delta) 30 ng/ml (BA.1) 2937 ng/ml (BA.2)	
(26)	W25-Fc			9.01 nM (WT) 0.38 nM (Alpha) 1.31 (Beta) 0.29 (Gamma) 1.45 nM (BA.1) 2.07 (BA.2)	Yes

WT: the original SARS-CoV-2 Wuhan strain isolated in early 2020

D614G: the original SARS-CoV-2 Wuhan strain with the added D614G mutation

References for Table S1:

1. **Wang L, Zhou T, Zhang Y, Yang ES, Schramm CA, Shi W, Pegu A, Oloniniyi OK, Henry AR, Darko S, Narpala SR, Hatcher C, Martinez DR, Tsybovsky Y, Phung E, Abiona OM, Antia A, Cale EM, Chang LA, Choe M, Corbett KS, Davis RL, DiPiazza AT, Gordon IJ, Hait SH, Hermanus T, Kgagudi P, Laboune F, Leung K, Liu T, Mason RD, Nazzari AF, Novik L, O'Connell S, O'Dell S, Olia AS, Schmidt SD, Stephens T, Stringham CD, Talana CA, Teng IT, Wagner DA, Widge AT, Zhang B, Roederer M, Ledgerwood JE, Ruckwardt TJ, Gaudinski MR, Moore PL, Doria-Rose NA, et al. 2021. Ultrapotent antibodies against diverse and highly transmissible SARS-CoV-2 variants. *Science* **373**.**
2. **Wang X, Hu A, Chen X, Zhang Y, Yu F, Yue S, Li A, Zhang J, Pan Z, Yang Y, Lin Y, Gao L, Zhou J, Zhao J, Li F, Shi Y, Huang F, Yang X, Peng Y, Tu L, Zhang H, Zheng H, He J, Zhang H, Xu L, Huang Q, Zhu Y, Deng K, Ye L. 2022. A potent human monoclonal antibody with pan-neutralizing activities directly dislocates S trimer of SARS-CoV-2 through binding both up and down forms of RBD. *Signal Transduct Target Ther* **7**:114.**
3. **Andreano E, Nicastrì E, Paciello I, Pileri P, Manganaro N, Piccini G, Manenti A, Pantano E, Kabanova A, Troisi M, Vacca F, Cardamone D, De Santi C, Torres JL, Ozorowski G, Benincasa L, Jang H, Di Genova C, Depau L, Brunetti J, Agrati C, Capobianchi MR, Castilletti C, Emiliozzi A, Fabbiani M, Montagnani F, Bracci L, Sautto G, Ross TM, Montomoli E, Temperton N, Ward AB, Sala C, Ippolito G, Rappuoli R. 2021. Extremely potent human monoclonal antibodies from COVID-19 convalescent patients. *Cell* **184**:1821-1835.e1816.**

4. **Yin W, Xu Y, Xu P, Cao X, Wu C, Gu C, He X, Wang X, Huang S, Yuan Q, Wu K, Hu W, Huang Z, Liu J, Wang Z, Jia F, Xia K, Liu P, Wang X, Song B, Zheng J, Jiang H, Cheng X, Jiang Y, Deng SJ, Xu HE.** 2022. Structures of the Omicron spike trimer with ACE2 and an anti-Omicron antibody. *Science* **375**:1048-1053.
5. **Wang X, Chen X, Tan J, Yue S, Zhou R, Xu Y, Lin Y, Yang Y, Zhou Y, Deng K, Chen Z, Ye L, Zhu Y.** 2022. 35B5 antibody potently neutralizes SARS-CoV-2 Omicron by disrupting the N-glycan switch via a conserved spike epitope. *Cell Host Microbe* **30**:887-895.e884.
6. **Zhou T, Wang L, Misasi J, Pegu A, Zhang Y, Harris DR, Olia AS, Talana CA, Yang ES, Chen M, Choe M, Shi W, Teng IT, Creanga A, Jenkins C, Leung K, Liu T, Stancofski ED, Stephens T, Zhang B, Tsybovsky Y, Graham BS, Mascola JR, Sullivan NJ, Kwong PD.** 2022. Structural basis for potent antibody neutralization of SARS-CoV-2 variants including B.1.1.529. *Science* **376**:eabn8897.
7. **Yao H, Sun Y, Deng YQ, Wang N, Tan Y, Zhang NN, Li XF, Kong C, Xu YP, Chen Q, Cao TS, Zhao H, Yan X, Cao L, Lv Z, Zhu D, Feng R, Wu N, Zhang W, Hu Y, Chen K, Zhang RR, Lv Q, Sun S, Zhou Y, Yan R, Yang G, Sun X, Liu C, Lu X, Cheng L, Qiu H, Huang XY, Weng T, Shi D, Jiang W, Shao J, Wang L, Zhang J, Jiang T, Lang G, Qin CF, Li L, Wang X.** 2021. Rational development of a human antibody cocktail that deploys multiple functions to confer Pan-SARS-CoVs protection. *Cell Res* **31**:25-36.
8. **Peng L, Hu Y, Mankowski MC, Ren P, Chen RE, Wei J, Zhao M, Li T, Tripler T, Ye L, Chow RD, Fang Z, Wu C, Dong MB, Cook M, Wang G, Clark P, Nelson B, Klein D, Sutton R, Diamond MS, Wilen CB, Xiong Y, Chen S.** 2022. Monospecific and bispecific monoclonal SARS-CoV-2 neutralizing antibodies that maintain potency against B.1.617. *Nat Commun* **13**:1638.
9. **Bertoglio F, Fühner V, Ruschig M, Heine PA, Abassi L, Klünemann T, Rand U, Meier D, Langreder N, Steinke S, Ballmann R, Schneider KT, Roth KDR, Kuhn P, Riese P, Schäckermann D, Korn J, Koch A, Chaudhry MZ, Eschke K, Kim Y, Zock-Emmenthal S, Becker M, Scholz M, Moreira G, Wenzel EV, Russo G, Garritsen HSP, Casu S, Gerstner A, Roth G, Adler J, Trimpert J, Hermann A, Schirrmann T, Dübel S, Frenzel A, Van den Heuvel J, Čičin-Šain L, Schubert M, Hust M.** 2021. A SARS-CoV-2 neutralizing antibody selected from COVID-19 patients binds to the ACE2-RBD interface and is tolerant to most known RBD mutations. *Cell Rep* **36**:109433.
10. **Dussupt V, Sankhala RS, Mendez-Rivera L, Townsley SM, Schmidt F, Wiczorek L, Lal KG, Donofrio GC, Tran U, Jackson ND, Zaky WI, Zemil M, Tritsch SR, Chen WH, Martinez EJ, Ahmed A, Choe M, Chang WC, Hajduczki A, Jian N, Peterson CE, Rees PA, Rutkowska M, Slike BM, Selverian CN, Swafford I, Teng IT, Thomas PV, Zhou T, Smith CJ, Currier JR, Kwong PD, Rolland M, Davidson E, Doranz BJ, Mores CN, Hatzioannou T, Reiley WW, Bieniasz PD, Paquin-Proulx D, Gromowski**

- GD, Polonis VR, Michael NL, Modjarrad K, Joyce MG, Krebs SJ.** 2021. Low-dose in vivo protection and neutralization across SARS-CoV-2 variants by monoclonal antibody combinations. *Nat Immunol* **22**:1503-1514.
11. **Wang K, Jia Z, Bao L, Wang L, Cao L, Chi H, Hu Y, Li Q, Zhou Y, Jiang Y, Zhu Q, Deng Y, Liu P, Wang N, Wang L, Liu M, Li Y, Zhu B, Fan K, Fu W, Yang P, Pei X, Cui Z, Qin L, Ge P, Wu J, Liu S, Chen Y, Huang W, Wang Q, Qin CF, Wang Y, Qin C, Wang X.** 2022. Memory B cell repertoire from triple vaccinees against diverse SARS-CoV-2 variants. *Nature* **603**:919-925.
 12. **Ye G, Gallant J, Zheng J, Massey C, Shi K, Tai W, Odle A, Vickers M, Shang J, Wan Y, Du L, Aihara H, Perlman S, LeBeau A, Li F.** 2021. The development of Nanosota-1 as anti-SARS-CoV-2 nanobody drug candidates. *Elife* **10**.
 13. **Xiang Y, Nambulli S, Xiao Z, Liu H, Sang Z, Duprex WP, Schneidman-Duhovny D, Zhang C, Shi Y.** 2020. Versatile and multivalent nanobodies efficiently neutralize SARS-CoV-2. *Science* **370**:1479-1484.
 14. **Schoof M, Faust B, Saunders RA, Sangwan S, Rezelj V, Hoppe N, Boone M, Billesbølle CB, Puchades C, Azumaya CM, Kratochvil HT, Zimanyi M, Deshpande I, Liang J, Dickinson S, Nguyen HC, Chio CM, Merz GE, Thompson MC, Diwanji D, Schaefer K, Anand AA, Dobzinski N, Zha BS, Simoneau CR, Leon K, White KM, Chio US, Gupta M, Jin M, Li F, Liu Y, Zhang K, Bulkley D, Sun M, Smith AM, Rizo AN, Moss F, Brilot AF, Pourmal S, Trenker R, Pospiech T, Gupta S, Barsi-Rhyne B, Belyy V, Barile-Hill AW, Nock S, Liu Y, Krogan NJ, Ralston CY, et al.** 2020. An ultrapotent synthetic nanobody neutralizes SARS-CoV-2 by stabilizing inactive Spike. *Science* **370**:1473-1479.
 15. **Huo J, Mikolajek H, Le Bas A, Clark JJ, Sharma P, Kipar A, Dormon J, Norman C, Weckener M, Clare DK, Harrison PJ, Tree JA, Buttigieg KR, Salguero FJ, Watson R, Knott D, Carnell O, Ngabo D, Elmore MJ, Fotheringham S, Harding A, Moynié L, Ward PN, Dumoux M, Prince T, Hall Y, Hiscox JA, Owen A, James W, Carroll MW, Stewart JP, Naismith JH, Owens RJ.** 2021. A potent SARS-CoV-2 neutralising nanobody shows therapeutic efficacy in the Syrian golden hamster model of COVID-19. *Nat Commun* **12**:5469.
 16. **Xu J, Xu K, Jung S, Conte A, Lieberman J, Muecksch F, Lorenzi JCC, Park S, Schmidt F, Wang Z, Huang Y, Luo Y, Nair MS, Wang P, Schulz JE, Tessarollo L, Bylund T, Chuang GY, Olia AS, Stephens T, Teng IT, Tsybovsky Y, Zhou T, Munster V, Ho DD, Hatzioannou T, Bieniasz PD, Nussenzweig MC, Kwong PD, Casellas R.** 2021. Nanobodies from camelid mice and llamas neutralize SARS-CoV-2 variants. *Nature* **595**:278-282.
 17. **Pymm P, Adair A, Chan LJ, Cooney JP, Mordant FL, Allison CC, Lopez E, Haycroft ER, O'Neill MT, Tan LL, Dietrich MH, Drew D, Doerflinger M, Dengler MA, Scott NE, Wheatley AK, Gherardin NA, Venugopal H, Cromer D, Davenport MP, Pickering R, Godfrey DI, Purcell DFJ, Kent SJ, Chung AW, Subbarao K,**

- Pellegrini M, Glukhova A, Tham WH.** 2021. Nanobody cocktails potently neutralize SARS-CoV-2 D614G N501Y variant and protect mice. *Proc Natl Acad Sci U S A* **118**.
18. **Ma H, Zhang X, Zheng P, Dube PH, Zeng W, Chen S, Cheng Q, Yang Y, Wu Y, Zhou J, Hu X, Xiang Y, Zhang H, Chiu S, Jin T.** 2022. Hetero-bivalent nanobodies provide broad-spectrum protection against SARS-CoV-2 variants of concern including Omicron. *Cell Res* **32**:831-842.
19. **Hong J, Kwon HJ, Cachau R, Chen CZ, Butay KJ, Duan Z, Li D, Ren H, Liang T, Zhu J, Dandey VP, Martin NP, Esposito D, Ortega-Rodriguez U, Xu M, Borgnia MJ, Xie H, Ho M.** 2022. Dromedary camel nanobodies broadly neutralize SARS-CoV-2 variants. *Proc Natl Acad Sci U S A* **119**:e2201433119.
20. **Xiang Y, Huang W, Liu H, Sang Z, Nambulli S, Tubiana J, Williams KL, Jr., Duprex WP, Schneidman-Duhovny D, Wilson IA, Taylor DJ, Shi Y.** 2022. Superimmunity by pan-sarbecovirus nanobodies. *Cell Rep* **39**:111004.
21. **Li W, Schäfer A, Kulkarni SS, Liu X, Martinez DR, Chen C, Sun Z, Leist SR, Drelich A, Zhang L, Ura ML, Berezuk A, Chittori S, Leopold K, Mannar D, Srivastava SS, Zhu X, Peterson EC, Tseng CT, Mellors JW, Falzarano D, Subramaniam S, Baric RS, Dimitrov DS.** 2020. High Potency of a Bivalent Human V(H) Domain in SARS-CoV-2 Animal Models. *Cell* **183**:429-441.e416.

Table S2. *In vivo* anti-SARS-CoV-2 potency of discovered antibodies in the literature

Reference	Nanobody	Conventional Antibody	Animal	Route	Treatment time (hpi)	Dosage (mg/kg)	Virus
Current study	Nanosota-2A-Fc		Mouse	IP	4	4 10	WT
					18	16	
Current study	Nanosota-3A-Fc		Mouse	IP	4	10	Omicron
(1)		35B5 32C7	Mouse	IP	6	20	WT
					4	30	614G, Beta, Delta
(2)		J08, I14	Hamster	IP	24	4	WT
(3)		P17	Mouse	IP	-12 (pre-)	20	WT
					4		
(4)		Clone2	Mouse	IP	-24 (pre-) 18	20	WT
		Clone6					Delta
		Clone13A					
(5)		STE90-C11	Mouse	IV	1	6 30 60 120	WT
			Hamster	IP	2	3.7 37	
(6)		WRAIR NTD mAbs	Mouse	IV	-24 (pre-)	0.25	WT
		WRAIR RBD mAbs				1	
		Cocktail				24	
(7)		31 RBD mAbs	Mouse	IP	1	5	Beta
					2	30	Omicron
(8)	Nanosota-1C-Fc		Mouse	IP	-24 (pre-)	20	WT
					4	10 20	
(9)	C5-Trimer		Hamster	IP	24	4	WT
(10)	WNb-Fc 36		Mouse	IP	-24 (pre-)	0.2	WT (N501Y D614G)
(11)	aRBD-2-5-Fc		Mouse	IP	-24 (pre-)	10	WT
			Hamster		-24 (pre-) 3		Omicron
(12)	8A2+7A3		Mouse	IP	-2 (pre-)	5	Beta

(13)	V _H -Fc ab8		Mouse	IP	-12 (pre-)	8 36	WT (Q498T/P499Y)
			Hamster		-24 (pre-) 6	10	WT
(14)	VHH72-Fc		Mouse	IP IN	-7 (pre-)	5 1	Muc-IMB-1/2020
	HumVHH S56A/LA LAPG- Fc/Gen2		Hamster	IP	-24 (pre-)	20	Beta
	(humVHH _S56A) ₂ /L ALAPG- Fc/Gen2				IP	4	
(15)	ShAb01 ShAb02		Mouse	IP	-24 (pre-)	10	
(16)	MR14		Mouse	IP IN	-6 (pre-)	5	BA.2
				IN (3 dose)	6, 30, 54		
				IP	6		
(17)	W25-Fc		Mouse	IP	-4 (pre-) 24	5	Beta
				IP	24	5	BA.1
				IN		1	

Pre-: time refers to hours pre-challenge

IP: intraperitoneally

IN: intranasally

IV: intravenously

References for Table S2:

1. **Wang X, Hu A, Chen X, Zhang Y, Yu F, Yue S, Li A, Zhang J, Pan Z, Yang Y, Lin Y, Gao L, Zhou J, Zhao J, Li F, Shi Y, Huang F, Yang X, Peng Y, Tu L, Zhang H, Zheng H, He J, Zhang H, Xu L, Huang Q, Zhu Y, Deng K, Ye L.** 2022. A potent human monoclonal antibody with pan-neutralizing activities directly dislocates S trimer of SARS-CoV-2 through binding both up and down forms of RBD. *Signal Transduct Target Ther* 7:114.
2. **Andreano E, Nicastri E, Paciello I, Pileri P, Manganaro N, Piccini G, Manenti A, Pantano E, Kabanova A, Troisi M, Vacca F, Cardamone D, De Santi C, Torres JL, Ozorowski G, Benincasa L, Jang H, Di Genova C, Depau L, Brunetti J, Agrati C, Capobianchi MR, Castilletti C, Emiliozzi A, Fabbiani M, Montagnani F, Bracci L, Sautto G, Ross TM, Montomoli E, Temperton N, Ward AB, Sala C, Ippolito G, Rappuoli R.** 2021. Extremely potent human monoclonal antibodies from COVID-19 convalescent patients. *Cell* 184:1821-1835.e1816.
3. **Yao H, Sun Y, Deng YQ, Wang N, Tan Y, Zhang NN, Li XF, Kong C, Xu YP, Chen Q, Cao TS, Zhao H, Yan X, Cao L, Lv Z, Zhu D, Feng R, Wu N, Zhang W, Hu Y,**

- Chen K, Zhang RR, Lv Q, Sun S, Zhou Y, Yan R, Yang G, Sun X, Liu C, Lu X, Cheng L, Qiu H, Huang XY, Weng T, Shi D, Jiang W, Shao J, Wang L, Zhang J, Jiang T, Lang G, Qin CF, Li L, Wang X. 2021. Rational development of a human antibody cocktail that deploys multiple functions to confer Pan-SARS-CoVs protection. *Cell Res* **31**:25-36.**
4. **Peng L, Hu Y, Mankowski MC, Ren P, Chen RE, Wei J, Zhao M, Li T, Tripler T, Ye L, Chow RD, Fang Z, Wu C, Dong MB, Cook M, Wang G, Clark P, Nelson B, Klein D, Sutton R, Diamond MS, Wilen CB, Xiong Y, Chen S. 2022. Monospecific and bispecific monoclonal SARS-CoV-2 neutralizing antibodies that maintain potency against B.1.617. *Nat Commun* **13**:1638.**
 5. **Bertoglio F, Fühner V, Ruschig M, Heine PA, Abassi L, Klünemann T, Rand U, Meier D, Langreder N, Steinke S, Ballmann R, Schneider KT, Roth KDR, Kuhn P, Riese P, Schäckermann D, Korn J, Koch A, Chaudhry MZ, Eschke K, Kim Y, Zock-Emmenthal S, Becker M, Scholz M, Moreira G, Wenzel EV, Russo G, Garritsen HSP, Casu S, Gerstner A, Roth G, Adler J, Trimpert J, Hermann A, Schirrmann T, Dübel S, Frenzel A, Van den Heuvel J, Čičin-Šain L, Schubert M, Hust M. 2021. A SARS-CoV-2 neutralizing antibody selected from COVID-19 patients binds to the ACE2-RBD interface and is tolerant to most known RBD mutations. *Cell Rep* **36**:109433.**
 6. **Dussupt V, Sankhala RS, Mendez-Rivera L, Townsley SM, Schmidt F, Wiczorek L, Lal KG, Donofrio GC, Tran U, Jackson ND, Zaky WI, Zemil M, Tritsch SR, Chen WH, Martinez EJ, Ahmed A, Choe M, Chang WC, Hajduczki A, Jian N, Peterson CE, Rees PA, Rutkowska M, Slike BM, Selverian CN, Swafford I, Teng IT, Thomas PV, Zhou T, Smith CJ, Currier JR, Kwong PD, Rolland M, Davidson E, Doranz BJ, Mores CN, Hatzioannou T, Reiley WW, Bieniasz PD, Paquin-Proulx D, Gromowski GD, Polonis VR, Michael NL, Modjarrad K, Joyce MG, Krebs SJ. 2021. Low-dose in vivo protection and neutralization across SARS-CoV-2 variants by monoclonal antibody combinations. *Nat Immunol* **22**:1503-1514.**
 7. **Wang K, Jia Z, Bao L, Wang L, Cao L, Chi H, Hu Y, Li Q, Zhou Y, Jiang Y, Zhu Q, Deng Y, Liu P, Wang N, Wang L, Liu M, Li Y, Zhu B, Fan K, Fu W, Yang P, Pei X, Cui Z, Qin L, Ge P, Wu J, Liu S, Chen Y, Huang W, Wang Q, Qin CF, Wang Y, Qin C, Wang X. 2022. Memory B cell repertoire from triple vaccinees against diverse SARS-CoV-2 variants. *Nature* **603**:919-925.**
 8. **Ye G, Gallant J, Zheng J, Massey C, Shi K, Tai W, Odle A, Vickers M, Shang J, Wan Y, Du L, Aihara H, Perlman S, LeBeau A, Li F. 2021. The development of Nanosota-1 as anti-SARS-CoV-2 nanobody drug candidates. *Elife* **10**.**
 9. **Huo J, Mikolajek H, Le Bas A, Clark JJ, Sharma P, Kipar A, Dormon J, Norman C, Weckener M, Clare DK, Harrison PJ, Tree JA, Buttigieg KR, Salguero FJ, Watson R, Knott D, Carnell O, Ngabo D, Elmore MJ, Fotheringham S, Harding A, Moynié L, Ward PN, Dumoux M, Prince T, Hall Y, Hiscox JA, Owen A, James W, Carroll MW, Stewart JP, Naismith JH, Owens RJ. 2021. A potent SARS-CoV-2 neutralising**

nanobody shows therapeutic efficacy in the Syrian golden hamster model of COVID-19. *Nat Commun* **12**:5469.

10. **Pymm P, Adair A, Chan LJ, Cooney JP, Mordant FL, Allison CC, Lopez E, Haycroft ER, O'Neill MT, Tan LL, Dietrich MH, Drew D, Doerflinger M, Dengler MA, Scott NE, Wheatley AK, Gherardin NA, Venugopal H, Cromer D, Davenport MP, Pickering R, Godfrey DI, Purcell DFJ, Kent SJ, Chung AW, Subbarao K, Pellegrini M, Glukhova A, Tham WH.** 2021. Nanobody cocktails potently neutralize SARS-CoV-2 D614G N501Y variant and protect mice. *Proc Natl Acad Sci U S A* **118**.
11. **Ma H, Zhang X, Zheng P, Dube PH, Zeng W, Chen S, Cheng Q, Yang Y, Wu Y, Zhou J, Hu X, Xiang Y, Zhang H, Chiu S, Jin T.** 2022. Hetero-bivalent nanobodies provide broad-spectrum protection against SARS-CoV-2 variants of concern including Omicron. *Cell Res* **32**:831-842.
12. **Hong J, Kwon HJ, Cachau R, Chen CZ, Butay KJ, Duan Z, Li D, Ren H, Liang T, Zhu J, Dandey VP, Martin NP, Esposito D, Ortega-Rodriguez U, Xu M, Borgnia MJ, Xie H, Ho M.** 2022. Dromedary camel nanobodies broadly neutralize SARS-CoV-2 variants. *Proc Natl Acad Sci U S A* **119**:e2201433119.
13. **Li W, Schäfer A, Kulkarni SS, Liu X, Martinez DR, Chen C, Sun Z, Leist SR, Drelich A, Zhang L, Ura ML, Berezuk A, Chittori S, Leopold K, Mannar D, Srivastava SS, Zhu X, Peterson EC, Tseng CT, Mellors JW, Falzarano D, Subramaniam S, Baric RS, Dimitrov DS.** 2020. High Potency of a Bivalent Human V(H) Domain in SARS-CoV-2 Animal Models. *Cell* **183**:429-441.e416.
14. **Schepens B, van Schie L, Nerinckx W, Roose K, Van Breedam W, Fijalkowska D, Devos S, Weyts W, De Cae S, Vanmarcke S, Lonigro C, Eeckhaut H, Van Herpe D, Borloo J, Oliveira AF, Catani JPP, Creytens S, De Vlieger D, Michielsen G, Marchan JCZ, Moschonas GD, Rossey I, Sedeyn K, Van Hecke A, Zhang X, Langendries L, Jacobs S, Ter Horst S, Seldeslachts L, Liesenborghs L, Boudewijns R, Thibaut HJ, Dallmeier K, Velde GV, Weynand B, Beer J, Schnepf D, Ohnemus A, Remory I, Foo CS, Abdelnabi R, Maes P, Kaptein SJF, Rocha-Pereira J, Jochmans D, Delang L, Peelman F, Staeheli P, Schwemmle M, Devoogdt N, et al.** 2021. An affinity-enhanced, broadly neutralizing heavy chain-only antibody protects against SARS-CoV-2 infection in animal models. *Sci Transl Med* **13**:eabi7826.
15. **Chen WH, Hajduczki A, Martinez EJ, Bai H, Matz H, Hill TM, Lewitus E, Chang WC, Dawit L, Peterson CE, Rees PA, Ajayi AB, Golub ES, Swafford I, Dussupt V, David S, Mayer SV, Soman S, Kuklis C, Corbitt C, King J, Choe M, Sankhala RS, Thomas PV, Zemil M, Wieczorek L, Hart T, Duso D, Kummer L, Yan L, Sterling SL, Laing ED, Broder CC, Williams JK, Davidson E, Doranz BJ, Krebs SJ, Polonis VR, Paquin-Proulx D, Rolland M, Reiley WW, Gromowski GD, Modjarrad K, Dooley H, Joyce MG.** 2023. Shark nanobodies with potent SARS-CoV-2 neutralizing activity and broad sarbecovirus reactivity. *Nat Commun* **14**:580.

16. **Liu H, Wu L, Liu B, Xu K, Lei W, Deng J, Rong X, Du P, Wang L, Wang D, Zhang X, Su C, Bi Y, Chen H, Liu WJ, Qi J, Cui Q, Qi S, Fan R, Jiang J, Wu G, Gao GF, Wang Q.** 2023. Two pan-SARS-CoV-2 nanobodies and their multivalent derivatives effectively prevent Omicron infections in mice. *Cell Rep Med* **4**:100918.
17. **Modhiran N, Lauer SM, Amarilla AA, Hewins P, Lopes van den Broek SI, Low YS, Thakur N, Liang B, Nieto GV, Jung J, Paramitha D, Isaacs A, Sng JDJ, Song D, Jorgensen JT, Cheuquemilla Y, Burger J, Andersen IV, Himelreichs J, Jara R, MacLoughlin R, Miranda-Chacon Z, Chana-Cuevas P, Kramer V, Spahn C, Mielke T, Khromykh AA, Munro T, Jones ML, Young PR, Chappell K, Bailey D, Kjaer A, Herth MM, Jurado KA, Schwefel D, Rojas-Fernandez A, Watterson D.** 2023. A nanobody recognizes a unique conserved epitope and potently neutralizes SARS-CoV-2 omicron variants. *iScience* **26**:107085.

Table S3: Cryo-EM data collection, refinement and validation statistics.

	Spike/2A complex with 2 RBDs up	Local refinement of Spike/2A complex with 2 RBDs up	Spike/3A complex with 2 RBDs up and 3 Nbs bound	Local refinement of Spike/3A complex with 2 RBDs up and 3 Nbs bound	Spike/3A complex with 1 RBD up and 2 Nbs bound	Local refinement of Spike/3A complex with 1 RBD up and 2 Nbs bound	Spike/4A complex with 2 RBDs up and 3 Nbs bound	Local refinement of spike/4A complex with 2 RBDs up and 3 Nbs bound
Data collection and processing								
Magnification	165,000		165,000		165,000		75,300	
Voltage (kV)	300		300		300		300	
Electron exposure (e ⁻ /Å ²)	40.00		40.00		40.00		50.00	
Defocus range (μm)	0.8–2.4		0.8–2.4		0.8–2.4		0.75–2.5	
Pixel size (Å)	0.73		0.73		0.73		0.664	
Symmetry imposed	C1		C1		C1		C1	
Initial particle images (no.)	486,437	486,437	189,794	189,794	189,794	189,794	68,226	68,226
Final particle images (no.)	451,926	25124	81,068	81,068	77,360	77,360	58,046	58,046
Map resolution (Å)	2.1	5.6	2.5	3.3	2.5	3.2	3.4	4.1
FSC threshold	0.143	0.143	0.143	0.143	0.143	0.143	0.143	0.143
Map resolution range (Å)	1.8–4.6	5-10	2.0–8.0	3.0-8.0	2.0–8.0	3.0-8.0	3.0-8.0	3.2-10
Refinement								
Initial model used (PDB code)	7TGX	7TGX	7TGX	7TGX	7TGX	7TGX	7TGX	7TGX
Model resolution (Å)	2.7	9.4	2.9	4.0	2.9	3.6	3.8	7.4
FSC threshold	0.5	0.5	0.5	0.5	0.5	0.5	0.5	0.5
Model resolution range (Å)	44.3-2.1	23.4-5.0	51.4-2.4	43.3-3.2	52.0-2.4	40.0-3.2	63.0-3.4	54.4-4.0
Map sharpening <i>B</i> factor (Å ²)	-44.9	-348.4	-43.2	-66.0	-42.7	-70.3	-81.2	-97.3
Model composition								
Non-hydrogen atoms	25761	3037	28420	16237	27543	15406	28711	17466
Protein residues	3217	338	3562	2046	3447	1928	3598	2193
Ligands	45		47	2	47	7	47	12
<i>B</i> factors (Å ²)								
Protein	106.09	228.15	128.96	173.60	129.02	126.74	159.30	144.99
Nucleotide								
Ligand	115.62		118.50	172.91	129.21	150.68	144.99	126.54
R.m.s. deviations								
Bond lengths (Å)	0.006	0.004	0.005	0.006	0.005	0.004	0.016	0.005
Bond angles (°)	0.949	0.852	0.843	0.831	0.839	0.724	1.028	0.767
Validation								
MolProbity score	2.33	1.78	2.17	2.18	2.09	1.96	1.81	2.04
Clashscore	32.58	15.75	21.22	24.55	20.71	14.00	14.17	17.42
Poor rotamers (%)	1.24	0.00	1.26	0.61	1.16	0.29	0.54	0.05
Ramachandran plot								
Favored (%)	96.20	97.64	95.97	95.65	96.48	95.59	97.19	95.68
Allowed (%)	3.45	2.36	3.77	4.10	3.37	4.25	2.70	4.09
Disallowed (%)	0.35	0.00	0.26	0.25	0.15	0.16	0.11	0.23

2A, 3A and 4A represent Nanosota-2A, -3A and -4A, respectively.